MRS Advances

Indirect versus direct 3D printing of hydrogel scaffolds for adipose tissue regeneration

Lana Van Damme[1], Emilie Briant[1], Phillip Blondeel[2], Sandra Van Vlierberghe[1]

1. Polymer Chemistry & Biomaterials Group – Centre of Macromolecular Chemistry (CMaC) – Gent Alliance for Tissue Engineering (GATE) – Department of Organic and Macromolecular Chemistry, Ghent University, Krijgslaan 281, S4-Bis, 9000 Ghent, Belgium.

2. Department of Plastic & Reconstructive Surgery, Ghent University Hospital, Corneel Heymanslaan 10, 2K12, 9000 Ghent, Belgium

There exists a need for an innovative reconstructive approach for breast reconstruction, tackling current drawbacks and limitations present in the clinic. In this respect, adipose tissue engineering could offer a promising alternative. We have previously shown that methacrylamide-functionalized gelatin scaffolds are suitable to support the adhesion of adipose tissue-derived stem cells as well as their subsequent differentiation into the adipogenic lineage. The current paper aims to compare different techniques to produce such scaffolds including direct versus indirect 3D printing. Extrusion-based (direct) 3D printing was compared to indirect 3D printing exploiting a polylactic acid (PLA) sacrificial mould, thereby focussing on the physico-chemical characteristics of the obtained scaffolds. The results indicate that similar properties can be achieved irrespective of the technique applied. It can therefore be concluded that indirect 3D printing could offer some benefits over direct additive manufacturing (AM) as a more complex design can be created while materials that were previously unsuited for direct printing because of limitations associated with their characteristics (e.g. low viscosity), could potentially be applied as starting materials for indirect 3D printing to generate porous constructs with full control over their design.

Corresponding author: Prof. Sandra Van Vlierberghe

INTRODUCTION:

Nowadays, breast implants, lipofilling and micro-surgical free tissue transfer are the most popular procedures to repair soft tissue defects resulting from mastectomies/lumpectomies following breast cancer. With breast cancer being the most common cancer affecting women worldwide, 2.1 million cases in 2018, there is a clinical need for reconstructive strategies addressing current drawbacks and limitations such as capsular contracture, 50-80% resorption rate upon lipofilling and microsurgical complications [1]–[3].

Adipose tissue engineering through additive manufacturing (AM) of biomimetic materials could offer a promising alternative as this enables the fabrication of a 3D extracellular matrix mimic of which geometry and pore size can be predefined [4].

One of the most crucial parameters to create such a micro-environment is the material selection, as biodegradability and biocompatibility are strict requirements. Gelatin, derived from denatured collagen, has received increasing attention during the last decade, owing to its inherent bioactivity [5]. Gelatin is suitable for promoting cell adhesion and proliferation, since it contains the Arg-Gly-Asp sequence which is able to bind with cell surface integrins [6], [7]. Cross-linkable functionalities are often incorporated to develop a stable, cross-linked hydrogel system with tuneable mechanical properties. One frequently reported material in the latter respect is methacrylamide-modified gelatin (GelMA) [8]. GelMA can subsequently be processed into scaffolds for further use. We have previously shown that methacrylamide-functionalized gelatin scaffolds are suitable to support the adhesion of adipose tissue-derived stem cells as well as their subsequent differentiation into the adipogenic lineage [9].

There exist several methods to create scaffolds including AM of a biomaterial. Currently, AM is considered the gold standard over the more conventional approaches, such as solvent casting as patient-specific scaffolds can be created. Indeed, thanks to a computer aided design (CAD), the scaffold architecture can be controlled and more intricate, patient-specific scaffolds can be designed [10], [11]. As a result, AM appears to enable superior control over cellular behaviour as a specific architecture will influence cell proliferation, differentiation and diffusion of nutrients, cells and waste [12], [13]. However, this approach still exhibits certain limitations. For example, in the case of nozzle-based systems, the design will be limited to the printer resolution and certain architectural designs might not even be printable at all. Indirect 3D printing could offer potential to develop a more intricate, complex 3D design circumventing geometrical and material-related (e.g. low viscosity) limitations posed by direct 3D printing of hydrogels [14]. First, a negative blueprint of the targeted construct needs to be designed. The sacrificial mould can then be printed via numerus high resolution devices, enabling the generation of well-defined scaffolds. The material is then casted and crosslinked into its final shape, before removal of the mould [15], [16].

The present work focusses on the physico-chemical differences between scaffolds developed via indirect 3D printing on the one hand and additive manufacturing through extrusion-based printing on the other hand. To the best of our knowledge, this is the first paper reporting on a comparative study of both techniques.

MATERIALS AND METHODS

Materials

Gelatin type B (Gel-B), isolated from bovine skin through an alkaline process was supplied by Rousselot (Ghent, Belgium). The Spectrapor dialysis membranes

(MWCO 12000-14000 g/mol) were supplied by Polylab (Antwerp, Belgium). Methacrylic anhydride, D_2O and ethylenediaminetetraacetic acid disodium salt (EDTA) were used as received from Sigma-Aldrich (Diegem, Belgium). Sodium phosphate (dibasic) and potassium phosphate (monobasic) and calcium chloride (96 %) ($CaCl_2$) were obtained from Acros (Geel, Belgium).

Development of methacrylamide-modified gelatin

A batch of GelMA was developed following a protocol reported earlier by Van Den Bulcke et al [17]. Briefly, 100 g gelatin (38.5 mmol amines), was dissolved in a 1 L phosphate buffer (0.1 M; pH 7.8) at 40 °C. After complete dissolution, 14.34 mL methacrylic anhydride (2.5 equivalents with respect to the primary amines, 96.25 mmol) were added under vigorous stirring. The reaction was allowed to react for 1h. Next, in order to remove the unreacted methacrylic anhydride and the methacrylic acid generated during modification, dialysis against distilled water was performed during 24h at 40 °C. Afterwards, the obtained GelMA was frozen at – 20 °C and lyophilized. The degree of substitution was determined using ^{1}H-NMR spectroscopy at 40 °C using D_2O in a Bruker WH 500 MHz NMR spectrometer.

Extrusion-based 3D printing

The porous scaffolds (10 x 10 x 10 mm²) were printed using an extrusion-based 3D Bioplotter (SysEng Bioscaffolder, Hünxe, Germany). To this end, an aqueous 10 w/v% GelMA solution was used containing 2 mol% (with respect to the methacrylamide moieties) of the photo-initiator Li-TPO-L. The solution was poured into a cartridge and subsequently physical crosslinking was realized by incubating the solution at 4°C during 30 min to obtain an increased viscosity. The obtained scaffolds were chemically crosslinked via UV-A irradiation (365 nm, 5 mW/cm^2) during 30 min.

Indirect 3D printing

PLA moulds were produced with the Ultimaker 3 (Ultimaker, Gerldermalsen, The Netherlands) via fused deposition modelling. A CAD design was developed mimicking a negative mould of the directly printed scaffolds which was printed via the Cura 13.06.4 software with a speed of 11 m/s at 210°C. As mentioned earlier, a 10 w/v% solution of GelMA was made in double distilled water (ddH_2O) with 2 mol% Li-TPO-L. Next, the PLA scaffolds were submerged in the GelMA solution at 40°C. To enable sufficient intrusion of GelMA solution inside the pores, the solution was placed under vacuum overnight, followed by chemical crosslinking through an optimized UV-A irradiation period of 1h30. Finally, in order to dissolve the PLA mould, the scaffolds were incubated in chloroform during 2 days under continuous stirring. The chloroform was changed twice a day.

Physico-chemical characterization

Gel fraction determination

The dry weight of the scaffolds was obtained after lyophilization. Next, the scaffolds were equilibrium swollen in ddH_2O at 37 °C for 24 h followed by lyophilization. The dry weight of the scaffolds was measured prior to and following swelling to calculate the gel fraction using the following formula:

Gel fraction (%)= (Wde/Wd0) x 100 (1)

Wd0 is the initial dry weight and Wde is the weight of the dried sample after 24h incubation. The calculations were performed on at least five scaffolds per material type.

Mass swelling ratio

The equilibrium mass swelling ratio was calculated by first incubating the scaffolds at 37 °C for 24h in double distilled water. The scaffolds were then weighed, lyophilized and weighed again to obtain the dry mass. The ratio was calculated using following formula:

Mass swelling ratio (q)= Ws/Wd (2)

Ws is the weight after 24h swelling at 37 °C and Wd is the dry weight following lyophilization.

Mechanical analysis of the scaffolds

A Tinius Olsen 5ST (Horsham, USA) was used to analyse the mechanical strength of the obtained scaffolds. First, scaffolds were equilibrium swollen in ddH_2O. A calliper was used to measure the dimensions of the swollen scaffolds. Next, the stress of the scaffolds was assessed using a load cell of 25N. The stress and strain were recorded at a constant speed of 10 mm/min. The Young's modulus was calculated via the slope of the first linear part of obtained plot.

Enzymatical degradation

The scaffolds were first lyophilized and the dry weight was measured. The samples were then submerged in a Tris-HCl buffer (0.1M, pH 7.4), containing 0.005 w/v% NaN_3 and 5 mM $CaCl_2$ and incubated for 1 hour at 37°C. After 1 hour, a collagenase solution (100CDU/ml Tris-HCl buffer) was added to the samples. Through addition of 0.1ml of a 0.25M EDTA solution, the degradation was stopped at different time points. The scaffolds were thoroughly washed in ice-cooled Tris-HCl buffer (three times) and ice-cooled double distilled water (three times). After lyophilization, the samples were weighed again, and the ratio of these weights was used to plot a degradation graph.

Statistical analysis

A two-tailed student t-test was performed when two average values were compared. If more values needed to be compared, statistical analysis was performed using a unifactorial analysis of variance (ANOVA). Two values were considered significantly different when the p-value was < 0.05.

RESULTS

Development of GelMA precursor

Methacrylamide moieties were introduced on the gelatin backbone, enabling subsequent UV-induced crosslinking in the presence of a photo-initiator. As indicated in the ^{1}H-NMR spectrum of the developed GelMA, the methacrylamide moieties were successfully introduced as can be observed from their characteristic peaks (5.6 and 5.8 ppm), as can be seen in Figure 1. The integrated intensities of these peaks were compared to these of the inert peaks of valine, leucine and isoleucine at 1.1 ppm to calculate the

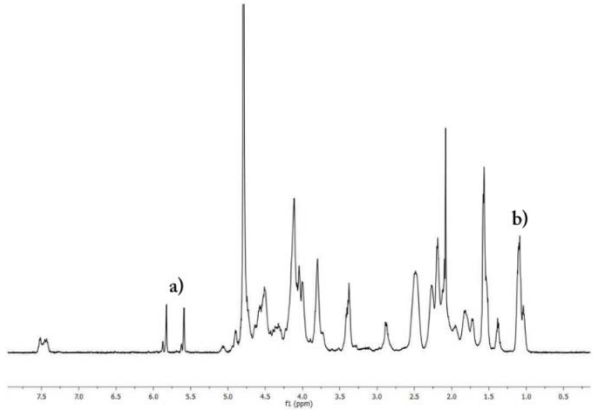

degree of substitution. The synthesis was successful as a DS of 97 was obtained which was around the targeted value.

Figure 1 ^{1}H-NMR spectrum of modified gelatin. The peaks corresponding with the protons of the methacrylamide functionalities are indicated with a. The peak that is marked with b corresponds with the methyl groups of valine, leucine and isoleucine.

Scaffold design

Extrusion-based 3D printing

Scaffolds constituting the developed GelMA were fabricated using extrusion-based 3D printing. The scaffolds were produced based on a cubical CAD design via layer-by-layer deposition. The printing parameters were optimized, resulting in the overview in Table I.

Table I: Overview of optimized printing parameters

Needle gauge	G27
Nozzle diameter	200 µm
Pore size	1.0 mm (0.8 - 1.3 mm)
Printing temperature	23 °C (22 - 28 °C)
Pressure	0.8 bar (0.6 - 1.3 bar)
XY speed	600 mm min^{-1} (400 - 700 mm min^{-1})
Z speed	650 mm min^{-1} (550 - 700 mm min^{-1})

Indirect 3D printing

Based on the obtained results of direct 3D printing, a CAD design was developed to act as a negative blueprint of the targeted scaffold dimensions, as depicted in Figure 2. The GelMA 10 w/v% solutions containing the photo-initiator were then casted in the moulds and fixed via UV-induced crosslinking, before removal of the sacrificial PLA mould via chloroform dissolution.

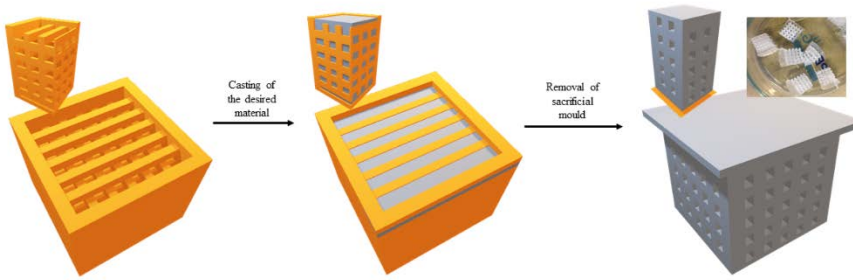

Figure 2. Scheme depicting indirect rapid prototyping process. From left to right: CAD design of the negative, sacrificial mould printed in PLA with a strut of 650µm and a pore size of 750 µm ; Casted material inside the mould; Obtained scaffolds after dissolving the mould in chloroform with a pore size of 650 µm and a strut size of 750µm.

Gel fraction and mass swelling determination

To obtain an indication of the crosslinking efficiency and stability of both scaffold types, a gel fraction assay was performed to determine the amount of insoluble material. Furthermore, the mass swelling ratio was also assessed as this enables to evaluate to what extent a hydrogel is able to mimic the aqueous environment of the extracellular matrix. The water uptake capacity and the gel fraction were measured comparing both directly and indirectly printed scaffolds. A gel fraction > 65% was obtained for both scaffolds (indirect 66.11 ± 1.13 and direct 71.23 ± 6.25) with a mass swelling ratio varying between 14-16. As can be seen in Figure 3, no significant differences could be observed, indicating that the mass swelling ratio and the gel fraction did not seem to differ between both techniques when similar scaffold dimensions are used.

Mechanical properties

A compression test was performed to gain insight in the mechanical properties of the scaffolds. Ideally, these scaffolds should mimic the mechanical strength of native fatty tissue, which is reported to be around 2 kPa [18]–[20]. The results show that similar young's moduli could be obtained varying between 1.36 ± 0.07 and 1.5 ± 0.30 for indirectly and directly printed scaffolds respectively, which is in the range of native fatty tissue. No significant differences could be observed between both scaffolds.

Enzymatic degradation

Lastly, to evaluate the enzymatic degradation of the scaffolds, a collagenase assay was performed. Here, similar observations were made, namely that there were no significant differences between the degradation behaviour of the directly and indirectly printed scaffolds. The scaffolds were almost fully degraded after 75min of incubation in a 100CDU/ml collagenase solution.

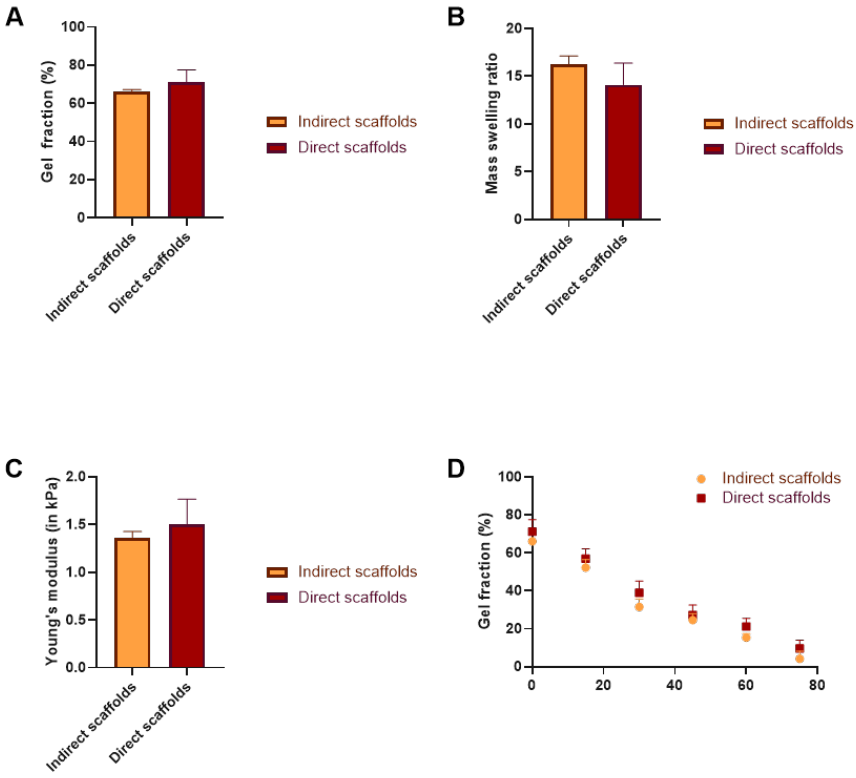

Figure 3. The physico-chemical properties of the printed scaffolds are depicted with: (A) Gel fraction; (B) Mass swelling ratio; (C) Young's modulus and (D) Enzymatic degradation.

DISCUSSION

This study targeted the comparison of two different techniques, namely AM and indirect rapid prototyping. In both cases, relatively low gel fractions were obtained. Due to the fact that the bottom of the sacrificial mould was a full layer of PLA, it was opted to only illuminate the scaffolds from the top as to minimize differences between both techniques. The low gel fraction can thus possibly be attributed to a limited UV-penetration. The UV-A light might not be able to penetrate completely to the bottom of the construct and light scattering might result in a decrease of the crosslinking efficiency. These observations are in agreement with the results obtained earlier by Shih et al. who demonstrated that thicker gels resulted in a decrease in crosslinking efficiency [21]. However, it needs to be stated that longer UV exposure times were used for the indirect scaffolds as it was hypothesized that the mould could interfere with UV-A penetration throughout the entire construct [16]. For the direct printed scaffolds, it was observed that longer UV exposure lead to dehydration of the scaffold. Hence, it was opted to perform exposure at the longest time possibly in which no dehydration was observed, which was 30 min.

Several studies have already reported on the mechanical strength of native breast, which is around 2 kPa [22]. The Young's moduli of the GelMA scaffolds were around 1.5

kPa. The structural density appeared to be similar, as there were no significant differences observed between both scaffold types. These results are in agreement with the gel fraction of the scaffolds

Through the use of a sacrificial mould, a more intricate design can potentially be developed. This could thus tackle the drawbacks currently posed by 3D printing of CAD designs limited by printer properties. Furthermore, materials that were previously limited through their own characteristics (e.g. low viscosity), could potentially be used to generate 3D constructs [23], [24]. In addition, it has already been reported in literature that low density gelatin scaffolds cannot be printed via conventional 3D processing without inducing collapse of the constructs. The limitations in processability of certain hydrogel precursor densities can thus become circumvented [8], [16].

There remain, however, some drawbacks that need to be tackled in the indirect 3D printing method to pave the way towards more advanced TE strategies. Currently, there are two different strategies in tissue engineering, namely the top-down and bottom-up approach. The conventional method is to seed cells onto an already built scaffold. The scaffold will degrade at a predictable rate, whilst the cells will proliferate and start to form their own ECM. There are some disadvantages associated with this approach, such as low mechanical support, slow vascularisation and inefficient cell colonization [25]–[29]. More recently, the bottom-up technique has gained more interest. Bottom-up TE has the potential to eliminate the drawbacks posed by the traditional top-down TE [30]. Instead of seeding cells on a pre-built scaffold, the cells are encapsulated before the cellular constructs are printed, rendering it a more modular technique. However, with the cells already being present during chemical crosslinking, free radicals can be detrimental [27], [29].

The longer UV exposure times and the use of chloroform only makes indirect 3D printing an ideal technique for the top-down tissue engineering approach during which cells are seeded on pre-built scaffolds. One of the solutions to circumvent this issue could be to use other materials then PLA as sacrificial mould material. In this respect, polyvinyl alcohol (PVA) could hold promise as a sacrificial mould as this can be washed away with water. To date, PVA is mostly used as a support material in fused deposition modelling [31]. It could therefore help to create a more suitable system for cell encapsulation purposes exploiting indirect 3D printing.

CONCLUSION

The current research paper reports on the physico-chemical properties of both indirectly and directly 3D printed scaffolds characterized by similar scaffold dimensions. For both printing techniques, the same material (methacrylamide-modified gelatin) was used. The results indicate that indirect 3D printing could potentially tackle the limitations that direct 3D printing poses (e.g. low viscosity materials cannot be processed) as no significant differences could be observed based on the physico-chemical properties (gel fraction, mass swelling ratio, mechanical properties and degradation time). The method allows for a straightforward and reproducible approach to create scaffolds that can further be used for tissue engineering applications with an even more intricate design.

ACKNOWLEDGMENTS

The authors would like to thank Mr. Tim Courtin for his help with recording the ^{1}H-NMR spectra. L. Van Damme would also like to acknowledge the Research Foundation Flanders (FWO) for providing her with an FWO-SB fellowship. S. Van Vlierberghe would

like to thank the FWO for financial support under the form of the research grant (G056219N).

References:

[1] F. Bray, Jacques Ferlay, Isabelle Soerjomataram, R. L. Siegel;, L. A. Torre;, and A. Jemal, "Global Cancer Statistics 2018: GLOBOCAN Estimates of Incidence and Mortality Worldwide for 36 Cancers in 185 Countries," *CA. Cancer J. Clin.*, 2018.

[2] A. Hassan El-Sabbagh, "Modern trends in lipomodelling," *GMS Interdiscip. Plast. Reconstr. Surg. DGPW*, vol. 6, no. April, 1998.

[3] J. Roostaeian, L. Pavone, A. Da Lio, J. Lipa, J. Festekjian, and C. Crisera, "Immediate placement of implants in breast reconstruction: Patient selection and outcomes," *Plast. Reconstr. Surg.*, vol. 127, no. 4, pp. 1407–1416, 2011.

[4] M. Vaezi, G. Zhong, H. Kalami, and S. Yang, "Extrusion-based 3D printing technologies for 3D scaffold engineering," *Mater. Technol. Appl.*, pp. 235–254, 2018.

[5] D. A. Young and K. L. Christman, "Injectable biomaterials for adipose tissue engineering," *Biomed. Mater.*, vol. 7, no. 2, pp. 1–17, 2012.

[6] E. Ruoslahti, "Rgd and Other Recognition Sequences for Integrins," *Annu. Rev. Cell Dev. Biol.*, vol. 12, no. 1, pp. 697–715, 1996.

[7] T. Chen, H. D. Embree, L. Q. Wu, and G. F. Payne, "In vitro protein-polysaccharide conjugation: Tyrosinase-catalyzed conjugation of gelatin and chitosan," *Biopolymers*, vol. 64, no. 6, pp. 292–302, 2002.

[8] T. Billiet, E. Gevaert, T. De Schryver, M. Cornelissen, and P. Dubruel, "The 3D printing of gelatin methacrylamide cell-laden tissue-engineered constructs with high cell viability," *Biomaterials*, vol. 35, no. 1, pp. 49–62, 2014.

[9] L. Tytgat *et al.*, "Additive manufacturing of photo-crosslinked gelatin scaffolds for adipose tissue engineering," *Acta Biomater.*, vol. 94, pp. 340–350, 2019.

[10] L. Flynn and K. A. Woodhouse, "Adipose tissue engineering with cells in engineered matrices," *Organogenesis*, vol. 4, no. 4, pp. 228–235, 2008.

[11] S. Peltola, F. Melchels, D. Grijpma, and M. Kellomäki, "A review of rapid prototyping techniques for tissue engineering purposes.," *Ann Med*, vol. 40, no. 4, pp. 268–80, 2008.

[12] C. Z. Liu, E. Sachlos, D. A. Wahl, Z. W. Han, and J. T. Czernuszka, "On the manufacturability of scaffold mould using a 3D printing technology," *Rapid Prototyp. J.*, 2007.

[13] M. Rumpler, A. Woesz, J. W. C. Dunlop, J. T. Van Dongen, and P. Fratzl, "The effect of geometry on three-dimensional tissue growth," *J. R. Soc. Interface*, 2008.

[14] J. Van Hoorick *et al.*, "(Photo-)crosslinkable gelatin derivatives for biofabrication applications," *Acta Biomater.*, 2019.

[15] C. De Maria, A. De Acutis, and G. Vozzi, "Indirect rapid prototyping for tissue engineering," in *Essentials of 3D Biofabrication and Translation*, 2015.

[16] J. Van Hoorick *et al.*, "Indirect additive manufacturing as an elegant tool for the production of self-supporting low density gelatin scaffolds," *J. Mater. Sci. Mater. Med.*, 2015.

[17] A. I. Van Den Bulcke, B. Bogdanov, N. De Rooze, E. H. Schacht, M. Cornelissen, and H. Berghmans, "Structural and rheological properties of methacrylamide modified gelatin hydrogels," *Biomacromolecules*, vol. 1, no. 1, pp. 31–38, 2000.

[18] D. Yoo, "New paradigms in hierarchical porous scaffold design for tissue engineering," *Mater. Sci. Eng. C*, vol. 33, no. 3, pp. 1759–1772, 2013.

[19] S. Ansari *et al.*, "Hydrogel elasticity and microarchitecture regulate dental-derived mesenchymal stem cell-host immune system cross-talk," *Acta Biomater.*, vol. 60, pp. 181–189, 2017.

[20] L. Tytgat *et al.*, "Additive manufacturing of photo-crosslinked gelatin scaffolds for adipose tissue engineering," *Acta Biomater.*, 2019.

[21] H. Shih, T. Greene, M. Korc, C. Lin, W. Lafayette, and B. Simon, "Modular and adaptable tumor niche prepared from visible light-initiated thiol-norbornene photopolymerization," vol. 17, no. 12, pp. 3872–3882, 2017.

[22] N. C. Negrini, P. Tarsini, M. C. Tanzi, and S. Farè, "Chemically crosslinked gelatin hydrogels as scaffolding materials for adipose tissue engineering," *J. Appl. Polym. Sci.*, vol. 47104, pp. 1–12, 2019.

[23] S. Hong *et al.*, "3D Printing of Highly Stretchable and Tough Hydrogels into Complex, Cellularized Structures," *Adv. Mater.*, 2015.

[24] J. Odent, T. J. Wallin, W. Pan, K. Kruemplestaedter, R. F. Shepherd, and E. P. Giannelis, "Highly Elastic, Transparent, and Conductive 3D-Printed Ionic Composite Hydrogels," *Adv. Funct. Mater.*, 2017.

[25] K. Hölzl, S. Lin, L. Tytgat, S. Van Vlierberghe, L. Gu, and A. Ovsianikov, "Bioink properties before, during and after 3D bioprinting," *Biofabrication*, vol. 8, pp. 1–19, 2016.

[26] A. Do, B. Khorsand, S. M. Geary, and A. K. Salem, "3D Printing of Scaffolds for Tissue Regeneration Applications," *Adv Heal. Mater*, vol. 4, no. 12, pp. 1742–1762, 2015.

[27] J. W. Nichol and A. Khademhosseini, "Modular tissue engineering: Engineering biological tissues from the bottom up," *Soft Matters*, vol. 5, no. 7, pp. 1312–1319, 2010.

[28] A. L. Rutz, K. E. Hyland, A. E. Jakus, W. R. Burghardt, and R. N. Shah, “A multimaterial bioink method for 3D printing tunable, cell-compatible hydrogels,” *Adv. Mater.*, vol. 27, no. 9, pp. 1607–1614, 2015.

[29] F. Urciuolo, G. Imparato, A. Totaro, and P. A. Netti, “Building a tissue in vitro from the bottom up: Implications in regenerative medicine.,” *Methodist Debakey Cardiovasc. J.*, vol. 9, no. 4, pp. 213–217, 2013.

[30] R. Tiruvannamalai-Annamalai, D. R. Armant, and H. W. T. Matthew, “A glycosaminoglycan based, modular tissue scaffold system for rapid assembly of perfusable, high cell density, engineered tissues,” *PLoS One*, vol. 9, no. 1, 2014.

[31] A. Goyanes, M. Kobayashi, R. Martínez-Pacheco, S. Gaisford, and A. W. Basit, “Fused-filament 3D printing of drug products: Microstructure analysis and drug release characteristics of PVA-based caplets,” *Int. J. Pharm.*, 2016.